applied sciences

MDPI

Article

New Methods of Series Expansions between Three Anomalies

Dongfang Zhao [1,*], Houpu Li [2], Shaofeng Bian [1], Yongbing Chen [1] and Wenkui Li [1]

[1] Department of Navigation Engineering, Naval University of Engineering, 717 Jiefang Avenue, Qiaokou District, Wuhan 430030, China; sfbian@sina.com (S.B.); hgcyb@163.com (Y.C.); lwk404@sjtu.edu.cn (W.L.)
[2] Department of Control Engineering, Naval University of Engineering, 717 Jiefang Avenue, Qiaokou District, Wuhan 430030, China; lihoupu1985@126.com
* Correspondence: 211804020003@home.hpu.edu.cn

Abstract: The calculation of satellite orbit involves some very complex formula derivations and expansions, which are very difficult to manually derive and prone to errors. And the efficiency of manual derivation is not high. We can use computer algebra systems to derive complex formulas related to satellite orbits. This can avoid some of the drawbacks of manual derivation and significantly improve computational efficiency and accuracy. In the past, the relationship among three anomalies was generally represented in the form of a trigonometric series with the first eccentricity e as the parameter. In this paper, the trigonometric series with the parameter $m = \frac{1-\sqrt{1-e^2}}{e}$ is used, as determined by the Lagrange conjugate series. We can use the formula of the Lagrange conjugate series to derive the relationship between the true anomaly and elliptic anomaly. And the relationship between the elliptic anomaly and the mean anomaly is derived by using the symbolic iteration method. In this research paper, we calculated the accuracy of the trigonometric series expansion among three types of anomalies at the first eccentricity e equal to values of 0.01, 0.1, and 0.2. The calculation results indicate that the accuracy of the trigonometric series expansion with m as the parameter is better than 10^{-5}. Moreover, in some cases, the trigonometric series expansion among the three anomalies with m as a parameter is simpler in form than the expansion expressed with parameter e. This paper also derived and calculated the symbolic expressions and extreme values of the difference among three anomalies and expressed the extreme values of the difference in the form of a power series of e. It can be seen that the extreme value increases with the increase in eccentricity e. And the absolute values of the extreme value of the difference between the elliptic anomaly and the mean anomaly, the true anomaly and the elliptic anomaly, and the true anomaly and the mean anomaly increase in this order. When the eccentricity is small, the absolute value of the extreme value of the difference between the true anomaly and the mean anomaly is about twice as large as the elliptic anomaly and the mean anomaly and the true anomaly and the mean anomaly.

Keywords: Lagrange conjugate series; anomaly; satellite orbit; Kepler's equation; symbolic iteration method; extreme value

Citation: Zhao, D.; Li, H.; Bian, S.; Chen, Y.; Li, W. New Methods of Series Expansions between Three Anomalies. *Appl. Sci.* **2024**, *14*, 3873. https://doi.org/10.3390/app14093873

Academic Editor: Atsushi Mase

Received: 24 March 2024
Revised: 24 April 2024
Accepted: 29 April 2024
Published: 30 April 2024

1. Introduction

With the development of the Chinese BeiDou Navigation Satellite System (BDS) globalization process, the construction of the third-generation BeiDou Navigation Satellite System with global coverage (BDS-3) was basically completed by the end of 2018 [1,2]. In 2020, China completed the global networking of the Beidou Navigation System and provided conventional PNT services as well as short message communication and international search and rescue services to global users [3]. The nominal space constellation of the Beidou-3 satellite consists of three geostationary orbit (GEO) satellites, three inclined geostationary orbit (IGSO) satellites, and twenty-four medium Earth orbit (MEO) satellites. Geostationary orbit (GEO) satellites have an orbit altitude of 35,786 km, located at 80 degrees east longitude, 110.5 degrees east longitude, and 140 degrees east longitude, respectively; the inclined geostationary orbit (IGSO) satellites have an orbit altitude of

35,786 km, and the inclination angle of the track surface is 55 degrees. The medium Earth orbit (MEO) satellites have an orbit altitude of 21,528 km, and the inclination angle of the track surface is 55 degrees. The Beidou Navigation Satellite System deploys in orbit backup satellites according to specific circumstances [4].

The Chinese space industry, represented by the BeiDou Navigation Satellite System (BDS), has developed vigorously and made great achievements [5,6]. With the needs of scientific research, business, and other aspects, more and more spacecrafts have been launched; most of these spacecrafts orbit the Earth. Some satellites, represented by the Beidou Navigation System, require the precise determination of their orbits [7,8]. And they may need to perform precise calculations on their orbital formulas, such as calculating satellite ephemeris. In these precise calculation processes, three types of anomalies of satellite orbits are often involved [9]. For example, in the process of converting the orbital elements to the vector of the position and velocity, the time element in the orbital elements is often used as the mean anomaly. But in the calculation, it needs to be converted to the true anomaly and the elliptic anomaly before calculation, which involves the transformation between the three types of anomalies. In addition, in many problems, it is necessary to express some parameters as explicit functions of time through the mean anomaly. However, due to the fact that Kepler's equation is a transcendental equation [10], it is difficult to obtain a rigorous analytical solution. We cannot directly convert the three types of anomalies. Many scholars have studied the Kepler equation. For example, M. K. Abubekerov et al. proposed a high-precision numerical solution for the Kepler equation [11]. Ruichen Zhang et al. solved Kepler's equation using the symbolic iteration method of computer algebra analysis [12]. Baisheng Wu et al. proposed a new analytical approach for constructing approximate solutions to the elliptic Kepler's equation [13]. In 1968, Karl Stumpff applied the Lie-Series to Kepler's problem of an undisturbed planet around the sun (two-body problem) [14]. R. H. Gooding and A. W. Odell proposed a method that solves the hyperbolic Kepler equation in a very efficient manner, and to an accuracy that proves to be always better than 10^{-20} [15]. Taking into account the monotony and convexity properties of the sine hyperbolic Kepler equation (SHK) and by making a detailed analysis of the discretization error, M. Calvo et al. provided a monotonic piecewise starter for this equation which has the q-convergence property for the Newton iteration [16]. M. Zechmeister developed an idea to solve Kepler's equation with a CORDIC-like algorithm, which solves Kepler's equation using only bitshifts, additions, and one initial multiplication [17]. O. González-Gaxiola and S. Hernández-Linares proposed a numerical technique, based on Banach's fixed-point theorem, to obtain an approximate solution of the elliptical Kepler equation [18]. Oliver H. E. Philcox et al. proposed an explicit integral solution, utilizing methods recently applied to the 'geometric goat problem' and to the dynamics of spherical collapse [19]. Danielle Tomasini and David N. Olivieri proposed two programs to solve Kepler's equation with high computational speed and optimal accuracy [20]. Furthermore, this also involves the conversion between three types of anomalies. The conversion expressions among the three types of anomalies are generally complex and extremely inconvenient in numerical calculations. We can express it in the form of series within an appropriate range of accuracy to improve its computational efficiency and accuracy [21].

With the application and development of space technology and computer technology in satellite ephemeris calculations, studying the relationship among the three types of anomalies of satellite motion (true anomaly, elliptic anomaly, and mean anomaly), as well as the extreme value problem of their differences, has a more important practical value. Many scholars at home and abroad have conducted in-depth research on the relationship among the three types of anomalies in satellite motion, but there are few studies in the literature that deeply analyze the extreme value problem of the differences among these three types of anomalies.

In this paper, we mainly use the Lagrange conjugate series to derive the series expansion formula between the true anomaly and the elliptic anomaly. Then, we derived the series expansion between the elliptic anomaly and the mean anomaly using the symbolic iteration method. We further use the series expansion between the true anomaly and the elliptic anomaly and the series expansion between the elliptic anomaly and the mean anomaly to derive the relationship between the true anomaly and the mean anomaly. And we analyze the accuracy and characteristics of the obtained expansion formulas. The expression derived in this paper is easy to compare and analyze. And the calculation results of this paper have, to some extent, expanded the scope of satellite motion analysis theory.

2. Materials and Methods

2.1. The Geometric Relationship among True Anomaly, Elliptic Anomaly, and Mean Anomaly

As shown in Figure 1, the point O is a focus of the satellite orbit ellipse. O' is the center of the ellipse. Point O' is the center of the circle. r is the radius vector of the satellite orbit. And the major half-axis of the ellipse is the radius of the auxiliary circle. S is the position of the satellite; perpendicular lines through S intersect H and extend the HS intersection auxiliary circle at S'. P is the perigee, f is the true anomaly, E is the elliptic anomaly, and M is the mean anomaly.

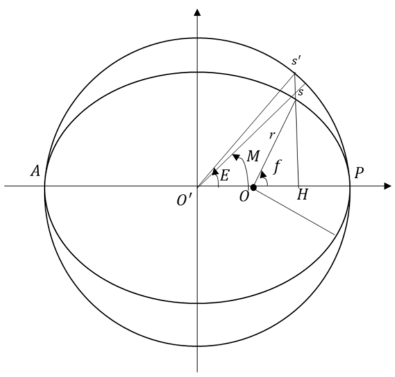

Figure 1. Schematic of the three types of anomalies.

It can be seen from Figure 1 that the coordinate expression of the satellite orbital radius vector r is as follows [22,23]:

$$\begin{cases} x = r\cos f = a\cos E - ae \\ y = r\sin f = a\sqrt{1-e^2}\sin E \end{cases} \tag{1}$$

In the above formula, parameter $e(e \ll 1)$ is the eccentricity of the satellite's elliptical orbit.

The relation between the radius vector r and the true anomaly f can be obtained from the polar equation of the ellipse [24,25]:

$$r = \frac{a\left(1-e^2\right)}{1+e\cos f} \tag{2}$$

The above formula can be transformed by shifting terms to obtain the following formula:

$$r\cos f = \frac{a\left(1-e^2\right)-r}{e} \tag{3}$$

The following formula can be obtained by combining the first equation of Formula (1) with Formula (3) [26,27]:

$$r = a - ae\cos E = a(1-e\cos E) \tag{4}$$

By substituting Formula (4) into Formula (1) and replacing the radius vector r, we can obtain the formula for calculating the true anomaly f from the elliptic anomaly E [28,29]:

$$\begin{cases} \cos f = \frac{\cos E - e}{1 - e\cos E} \\ \sin f = \frac{\sqrt{1-e^2}\sin E}{1 - e\cos E} \end{cases} \tag{5}$$

From Formula (5), we can also obtain the formula for calculating the elliptic anomaly E from the true anomaly f:

$$\begin{cases} \cos E = \frac{\cos f + e}{1 + e\cos f} \\ \sin E = \frac{\sqrt{1-e^2}\sin f}{1 + e\cos f} \end{cases} \tag{6}$$

From Formula (5), we can also derive the formula for the relationship between the true anomaly and the elliptic anomaly [30,31]:

$$\begin{aligned} \tan\frac{f}{2} &= \sqrt{\frac{1-\cos f}{1+\cos f}} = \sqrt{\frac{(1+e)(1-\cos E)}{(1-e)(1+\cos E)}} \\ &= \sqrt{\frac{1+e}{1-e}}\tan\frac{E}{2} \end{aligned} \tag{7}$$

The relationship between the mean anomaly M and the elliptic anomaly E is determined by Kepler's equation [32,33]:

$$M = E - e\sin E \tag{8}$$

2.2. The Derivation of the Expansion Formula for the Relationship between True Anomaly and Elliptic Anomaly

The essence of the Lagrange conjugate series is the series expansion of the tangent relationship between two variables [34]. The definition of the Lagrange conjugate series is as follows.

If there are two variables with the following relationship,

$$\tan y = K\tan x \tag{9}$$

Then, there can be the following relationship:

$$y - x = \frac{K-1}{K+1}\sin 2y - \frac{1}{2}\left(\frac{K-1}{K+1}\right)^2 \sin 4y + \frac{1}{3}\left(\frac{K-1}{K+1}\right)^3 \sin 6y \cdots \tag{10}$$

Alternatively, there can also be the following forms:

$$y - x = \frac{K-1}{K+1}\sin 2x + \frac{1}{2}\left(\frac{K-1}{K+1}\right)^2 \sin 4x + \frac{1}{3}\left(\frac{K-1}{K+1}\right)^3 \sin 6x \cdots \tag{11}$$

According to Formula (7) of the relationship between the true anomaly and the elliptic anomaly and the formula of the Lagrange conjugate series, let $\sqrt{\frac{1+e}{1-e}} = K$, $\frac{K-1}{K+1} = m$, and then we can obtain the following two Formulas (12) and (13):

$$\frac{f}{2} - \frac{E}{2} = m\sin f - \frac{1}{2}m^2\sin 2f + \frac{1}{3}m^3\sin 3f \cdots \tag{12}$$

$$\frac{f}{2} - \frac{E}{2} = m\sin E + \frac{1}{2}m^2\sin 2E + \frac{1}{3}m^3\sin 3E \cdots \tag{13}$$

We can further derive the following formulas by simply deriving the two Formulas (12) and (13) above:

$$E = f - 2\sum_{p=1}^{\infty}(-1)^{p+1}\frac{1}{p}m^p\sin pf \tag{14}$$

$$f = E + 2\sum_{p=1}^{\infty}\frac{1}{p}m^p\sin pE \tag{15}$$

In Formulas (14) and (15),

$$m = \frac{1-\sqrt{1-e^2}}{e} \tag{16}$$

By substituting Equations (16) into Equations (14) and (15), respectively, we can obtain the trigonometric series expansion formula with eccentricity e as the parameter. In the case where e is equal to zero, we expand the elliptic anomaly E and the true anomaly f into a power series form of eccentricity e. We take the expanded formulas to the e^8 terms to obtain Equations (17) and (18),

$$E = f + \sum_{n=1}^{8} a_n \sin nf \tag{17}$$

$$f = E + \sum_{n=1}^{8} b_n \sin nE \tag{18}$$

The coefficients in Formulas (17) and (18) are as follows:

$$\begin{cases} a_1 = -e - \frac{e^3}{4} - \frac{e^5}{8} - \frac{5e^7}{64} \\ a_2 = \frac{e^2}{4} + \frac{e^4}{8} + \frac{5e^6}{64} + \frac{7e^8}{128} \\ a_3 = -\frac{e^3}{12} - \frac{e^5}{16} - \frac{3e^7}{64} \\ a_4 = \frac{e^4}{32} + \frac{e^6}{32} + \frac{7e^8}{256} \\ a_5 = -\frac{e^5}{80} - \frac{e^7}{64} \\ a_6 = \frac{e^6}{192} + \frac{e^8}{128} \\ a_7 = -\frac{e^7}{448} \\ a_8 = \frac{e^8}{1024} \end{cases} \tag{19}$$

$$\begin{cases} b_1 = e + \frac{e^3}{4} + \frac{e^5}{8} + \frac{5e^7}{64} \\ b_2 = \frac{e^2}{4} + \frac{e^4}{8} + \frac{5e^6}{64} + \frac{7e^8}{128} \\ b_3 = \frac{e^3}{12} + \frac{e^5}{16} + \frac{3e^7}{64} \\ b_4 = \frac{e^4}{32} + \frac{e^6}{32} + \frac{7e^8}{256} \\ b_5 = \frac{e^5}{80} + \frac{e^7}{64} \\ b_6 = \frac{e^6}{192} + \frac{e^8}{128} \\ b_7 = \frac{e^7}{448} \\ b_8 = \frac{e^8}{1024} \end{cases} \tag{20}$$

2.3. The Derivation of the Expansion Formula for the Relationship between Elliptic Anomaly and Mean Anomaly

By shifting the terms of Kepler's Equation (8), we can obtain the following symbolic iterative relationship (14) [35]:

$$E = M + e \sin E \tag{21}$$

Due to the small difference between the elliptic anomaly E and the mean anomaly M, the initial value E_0 of the elliptic anomaly E can be taken as $E_0 = M$. By substituting the initial value E_0 of the elliptic anomaly into Formula (21), we can obtain the first iteration value E_1 of the elliptic anomaly:

$$E_1 = M + e \sin E_0 \tag{22}$$

By substituting the first iteration value E_1 of the elliptic anomaly into Kepler's Equation (21) for the second iteration, we expand the formula to the 8th order of e (If you want to improve computational accuracy, you need to expand to a higher order of e). We can obtain the second iteration result of the elliptic anomaly as follows:

$$E_2 = M + e \sin E_1 \tag{23}$$

The second iteration value E_2 of the elliptic anomaly is substituted into Kepler's Equation (21) to continue the iteration. Through calculation, we found that when the iteration formula for the elliptic anomaly is iterated for the ninth time, the coefficients of the formula no longer change. Then, the iteration of the formula stops. We can obtain the result of the ninth iteration, which is the trigonometric series expansion of the elliptic anomaly we obtained.

$$E_9 = M + \sum_{n=1}^{8} c_n \sin nM \tag{24}$$

$$\begin{cases} c_1 = e - \frac{e^3}{8} + \frac{e^5}{192} - \frac{e^7}{9216} \\ c_2 = \frac{e^2}{2} - \frac{e^4}{6} + \frac{e^6}{48} - \frac{e^8}{720} \\ c_3 = \frac{3e^3}{8} - \frac{27e^5}{128} + \frac{243e^7}{5120} \\ c_4 = \frac{e^4}{3} - \frac{4e^6}{15} + \frac{4e^8}{45} \\ c_5 = \frac{125e^5}{384} - \frac{3125e^7}{9216} \\ c_6 = \frac{27e^6}{80} - \frac{243e^8}{560} \\ c_7 = \frac{16807e^7}{46080} \\ c_8 = \frac{128e^8}{315} \end{cases} \tag{25}$$

We substitute $e = \frac{2m}{1+m^2}$ into Formula (24), and then we can obtain new coefficients in the form of m power series:

$$\begin{cases} c_1 = 2m - 3m^3 + \frac{31m^5}{6} - \frac{637m^7}{72} \\ c_2 = 2m^2 - \frac{20m^4}{3} + 18m^6 - \frac{1936m^8}{45} \\ c_3 = 3m^3 - \frac{63m^5}{4} + \frac{2313m^7}{40} \\ c_4 = \frac{16m^4}{3} - \frac{192m^6}{5} + \frac{8032m^8}{45} \\ c_5 = \frac{125m^5}{12} - \frac{6875m^7}{72} \\ c_6 = \frac{108m^6}{5} - \frac{8424m^8}{35} \\ c_7 = \frac{16807m^7}{360} \\ c_8 = \frac{32768m^8}{315} \end{cases} \tag{26}$$

Comparison of Efficiency

All algorithms were implemented in Python and run on a Lenovo XiaoXinPro 14IHU 2021 with a 4-core 3.11 GHz Intel i5-11300H processor. The manufacturer of the computer is Lenovo (Beijing) Co., Ltd., located in Beijing, China.

According to the literature, it is known that Kepler's Goat Herd is superior to the Newton–Raphson, Danby (1988), and Series methods [36,37]. Therefore, this article compares Kepler's Goat Herd method. The method in this article is only applicable to situations where $e \ll 1$.

Computation time (in milliseconds) required Kepler's equation to be solved for 10^6 points (equally spaced in E) using Kepler's Goat Herd and that of this work. The number of N was chosen by repeating the calculation until a mean absolute error below 10^{-12} (relative to the true solution) was obtained for the sample. We can find that when $e \ll 1$, the efficiency of the two methods has their own advantages and disadvantages. The comparison results are shown in Table 1.

Table 1. Comparison of efficiency between two methods.

Method	***e* = 0.01**		***e* = 0.05**		***e* = 0.1**		***e* = 0.2**	
	N	**Time**	***N***	**Time**	***N***	**Time**	***N***	**Time**
Kepler's Goat Herd	3	137.5	5	269.3	5	249.2	5	219.3
This Work	5	114.6	8	155.6	11	194.4	18	299.0

2.4. The Derivation of the Expansion Formula for the Relationship between True Anomaly and Mean Anomaly

By substituting Formula (14) into Formula (8), we can obtain the trigonometric series expression between the mean anomaly M and the true anomaly f. Then, around $m = 0$, we expand the obtained formula into a power series of m. We expand the formula to m^8.

$$M = f + \sum_{n=1}^{8} d_n \sin nf \tag{27}$$

$$\begin{cases} d_1 = -4m + 4m^3 - 4m^5 + 4m^7 \\ d_2 = 3m^2 - 4m^4 + 4m^6 - \frac{22m^8}{5} \\ d_3 = -\frac{8m^3}{3} + 4m^5 - \frac{18m^7}{5} \\ d_4 = \frac{5m^4}{2} - \frac{22m^6}{5} + \frac{24m^8}{5} \\ d_5 = -2m^5 + \frac{16m^7}{5} \\ d_6 = \frac{29m^6}{15} - \frac{16m^8}{5} \\ d_7 = -\frac{66}{35}m^7 \\ d_8 = \frac{8}{5}m^8 \end{cases} \tag{28}$$

If the eccentricity e is taken as the parameter, the coefficient of the formula is as follows:

$$\begin{cases} d_1 = -2e \\ d_2 = \frac{3e^2}{4} + \frac{e^4}{8} + \frac{3e^6}{64} + \frac{3e^8}{128} \\ d_3 = -\frac{e^3}{3} - \frac{e^5}{8} - \frac{e^7}{16} \\ d_4 = \frac{5e^4}{32} + \frac{3e^6}{32} + \frac{15e^8}{256} \\ d_5 = -\frac{3e^5}{40} - \frac{e^7}{16} \\ d_6 = \frac{7e^6}{192} + \frac{5e^8}{128} \\ d_7 = -\frac{e^7}{56} \\ d_8 = \frac{e^8}{128} \end{cases} \tag{29}$$

By substituting Formula (15) into Formula (24), we can obtain the trigonometric series expression between the true anomaly f and the mean anomaly M. Then, around $m = 0$, we expand the obtained formula into a power series of m. We expand the formula to m^8.

$$f = M + \sum_{n=1}^{8} g_n \sin nM \tag{30}$$

$$\begin{cases} g_1 = 4m - 6m^3 + \frac{35}{3}m^5 - \frac{769}{36}m^7 \\ g_2 = 5m^2 - \frac{52}{3}m^4 + 50m^6 - \frac{5644}{45}m^8 \\ g_3 = \frac{26}{3}m^3 - \frac{95}{2}m^5 + \frac{733}{4}m^7 \\ g_4 = \frac{103}{6}m^4 - \frac{644}{5}m^6 + \frac{28084}{45}m^8 \\ g_5 = \frac{1097}{30}m^5 - \frac{12539}{36}m^7 \\ g_6 = \frac{1223}{15}m^6 - \frac{32948}{35}m^8 \\ g_7 = \frac{47273}{252}m^7 \\ g_8 = \frac{556403}{1260}m^8 \end{cases} \tag{31}$$

If the eccentricity e is taken as the parameter, the coefficient of the formula is as follows:

$$\begin{cases} g_1 = 2e - \frac{e^3}{4} + \frac{5e^5}{96} + \frac{107e^7}{4608} \\ g_2 = \frac{5e^2}{4} - \frac{11e^4}{24} + \frac{17e^6}{192} + \frac{43e^8}{5760} \\ g_3 = \frac{13e^3}{12} - \frac{43e^5}{64} + \frac{95e^7}{512} \\ g_4 = \frac{103e^4}{96} - \frac{451e^6}{480} + \frac{4123e^8}{11520} \\ g_5 = \frac{1097e^5}{960} - \frac{5957e^7}{4608} \\ g_6 = \frac{1223e^6}{960} - \frac{7913e^8}{4480} \\ g_7 = \frac{47273e^7}{32256} \\ g_8 = \frac{556403e^8}{322560} \end{cases} \tag{32}$$

2.5. Error Analysis

In order to analyze the error of the series expansion obtained above, the value E_0 of the elliptic anomaly is given first. Then, we substitute the given value E_0 of the elliptic anomaly into Formula (7) to obtain the value f_0 of the true anomaly. We substitute the value E_0 of the elliptic anomaly into Kepler's Equation (8) to obtain the value M_0 of the mean anomaly. We take the values of the elliptic anomaly E_0, the true anomaly f_0, and the mean anomaly as theoretical values. By substituting the value E_0 of the elliptic anomaly into Formula (18), we can obtain the calculated value f_1 of the true anomaly. By substituting the value f_0 of the true anomaly into Formulas (17) and (27), we can obtain the calculated values E_1 of the elliptic anomaly and M_1 of the mean anomaly. By substituting the value M_0 of the mean anomaly into Formulas (24) and (30), we can obtain the calculated values E_2 of the elliptic anomaly and f_2 of the true anomaly. By subtracting the calculated values f_1, E_1, M_1, E_2, and f_2 of the three types of anomalies from the theoretical values E_0, f_0, and M_0, we can obtain the error of the trigonometric series expansion formula with e and m as parameters, respectively. We record the errors obtained above as Δf_1, ΔE_1, ΔM_1, ΔE_2 and Δf_2, respectively. When $e = 0.01$, $e = 0.1$, and $e = 0.2$, we draw error variation graphs for Δf_1, ΔE_1, ΔM_1, ΔE_2 and Δf_2, respectively [38].

From Figures 2–7 and Table 2, the following conclusions can be drawn:

1. These errors of the trigonometric series expansion of the three anomalies increase with the increase in eccentricity e.
2. These error plots of the trigonometric series expansions with parameters m and e for three anomalies are different, but they all exhibit central symmetry.
3. When $e = 0.01$, these errors Δf_1, ΔE_1, ΔM_1, ΔE_2, and Δf_2 calculated with parameter m are better than 10^{-15}. When $e = 0.1$, these errors are better than 10^{-7}. When $e = 0.2$, these errors are better than 10^{-5}.
4. When $e = 0.01$, these errors Δf_1, ΔE_1, ΔM_1, ΔE_2, and Δf_2 calculated with parameter e are better than 10^{-15}. When $e = 0.1$, these errors are better than 10^{-8}. When $e = 0.2$, the errors are better than 10^{-5}.
5. The transformation formula between the true anomaly f and the elliptic anomaly E with the parameter m is simpler in form than the formula with the parameter e.
6. The transformation formula between the true anomaly f and the mean anomaly M with the parameter m is simpler in form than the formula with the parameter e.

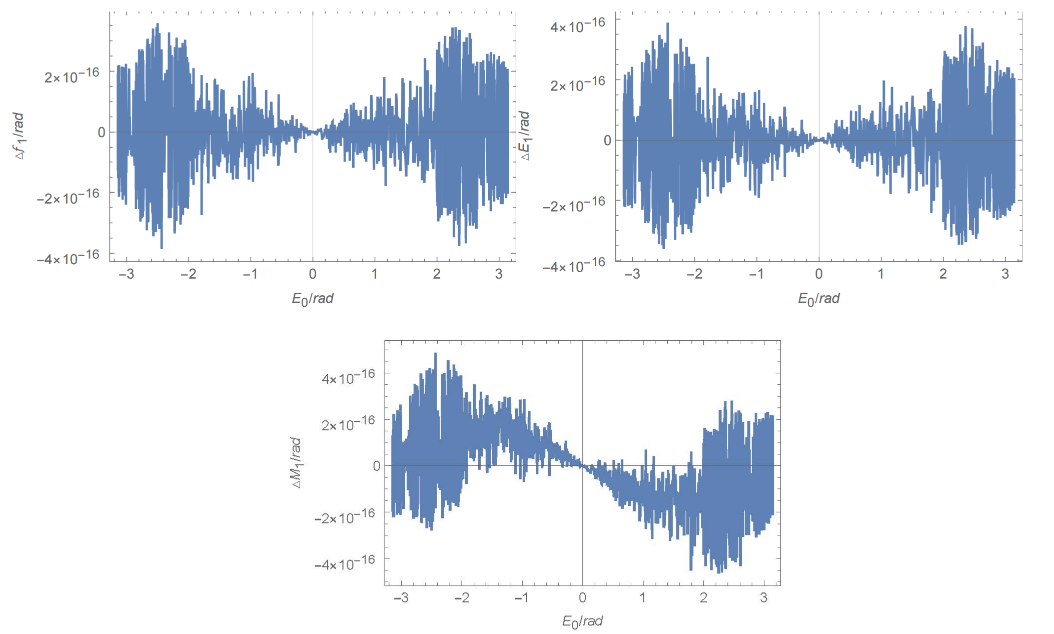

Figure 2. *Cont.*

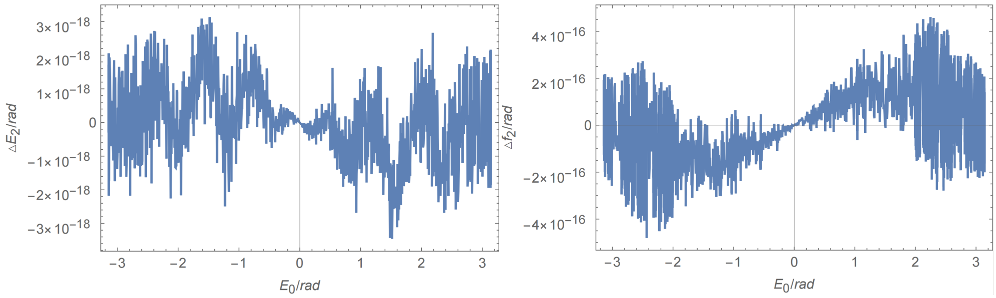

Figure 2. When $e = 0.01$ and the parameter of the expansion formula is m, the error varies with the elliptic anomaly E_0.

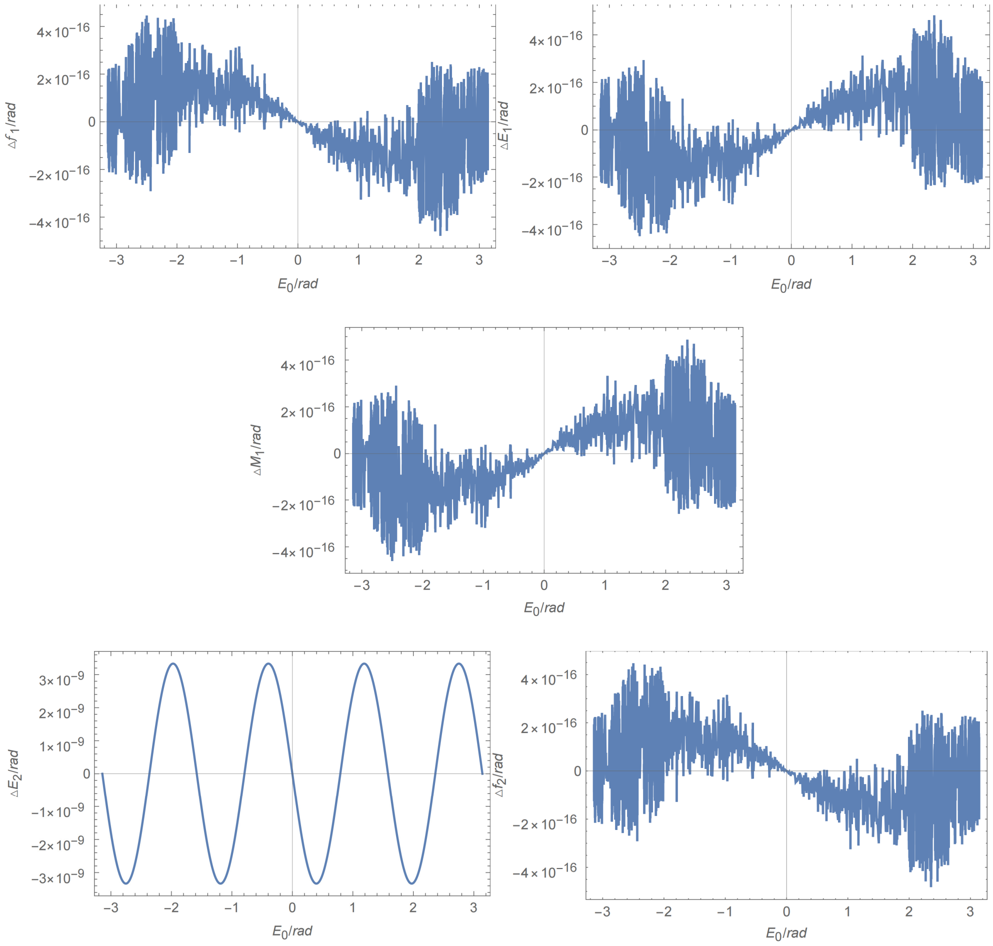

Figure 3. When $e = 0.01$ and the parameter of the expansion formula is e, the error varies with the elliptic anomaly E_0.

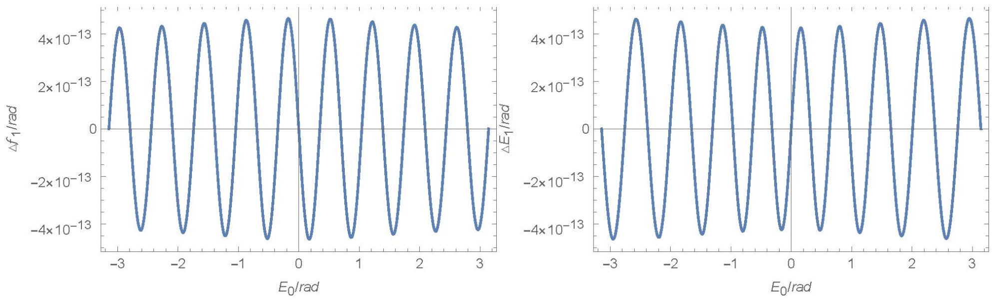

Figure 4. *Cont.*

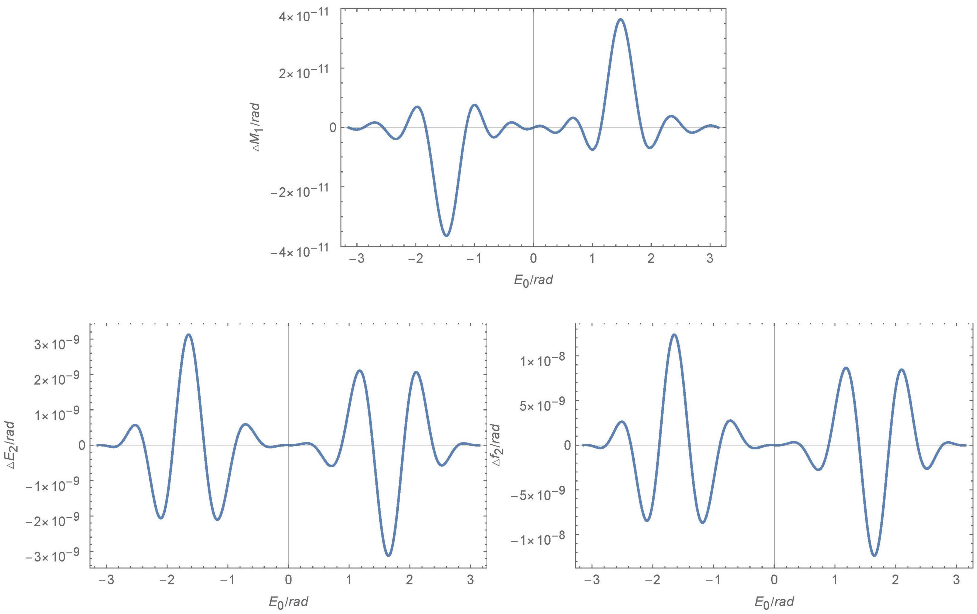

Figure 4. When $e = 0.1$ and the parameter of the expansion formula is m, the error varies with the elliptic anomaly E_0.

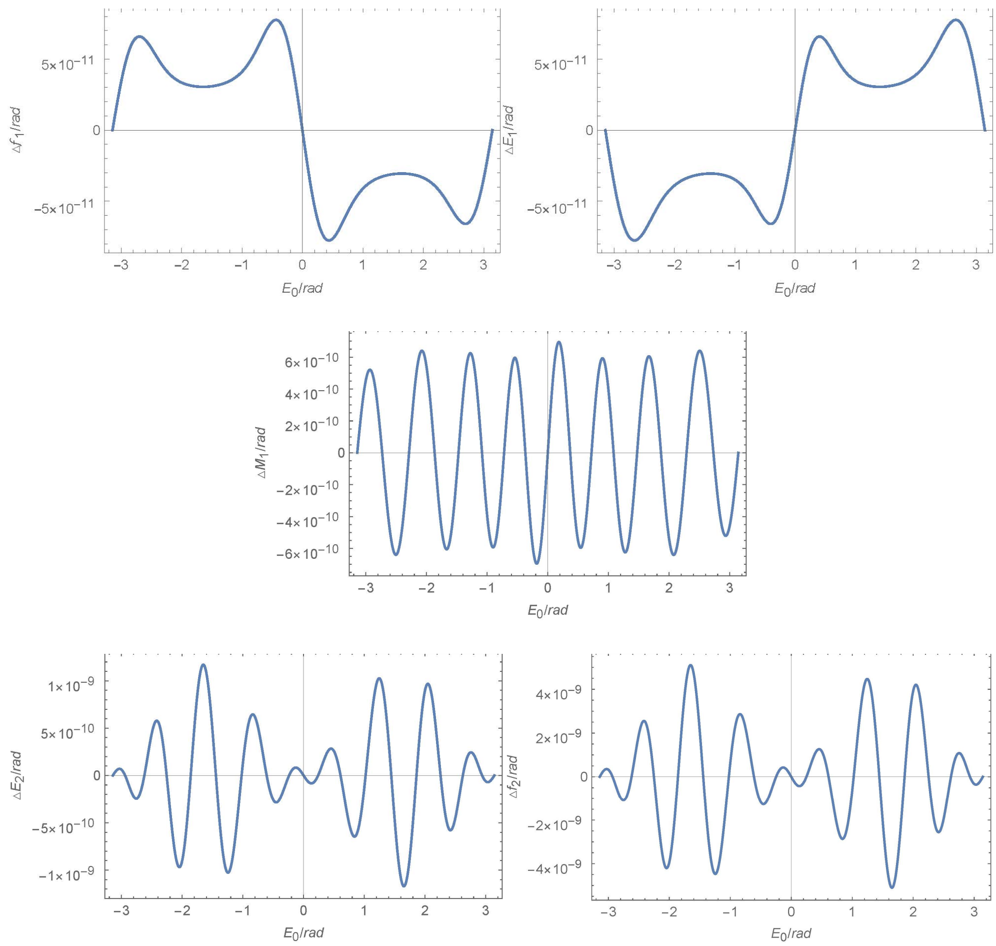

Figure 5. When $e = 0.1$ and the parameter of the expansion formula is e, the error varies with the elliptic anomaly E_0.

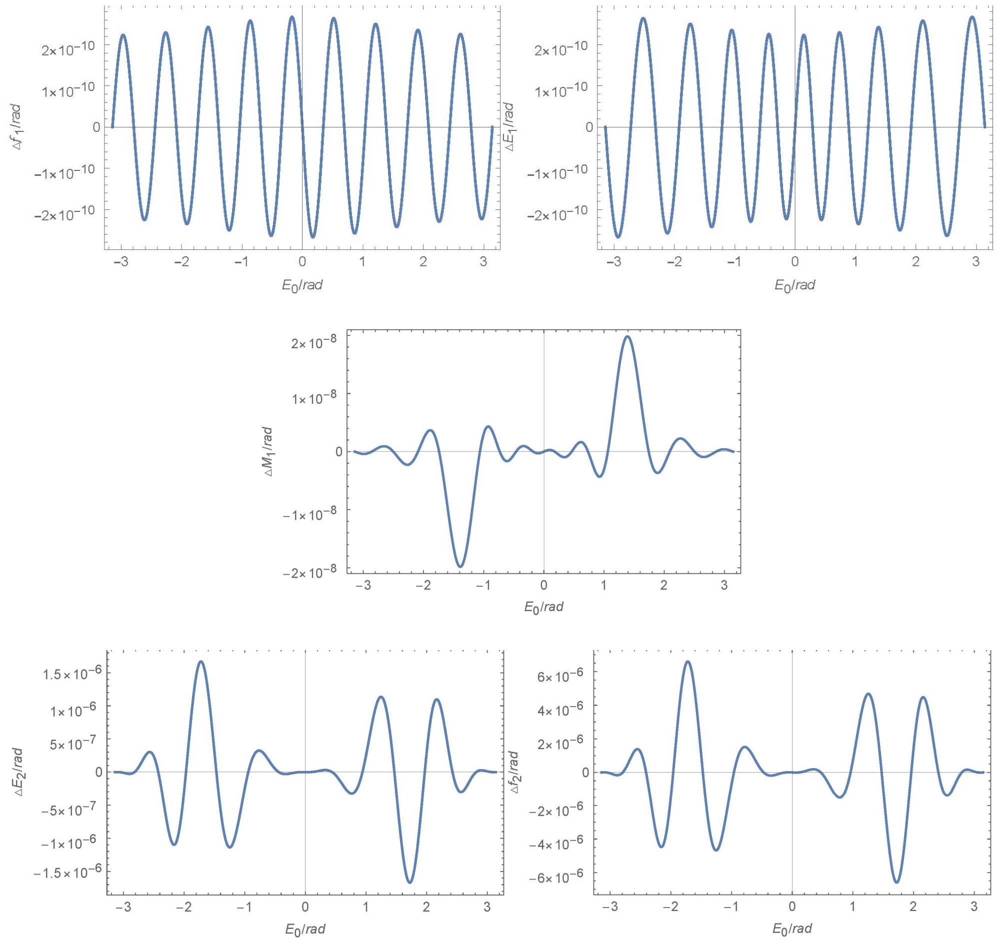

Figure 6. When $e = 0.2$ and the parameter of the expansion formula is m, the error varies with the elliptic anomaly E_0.

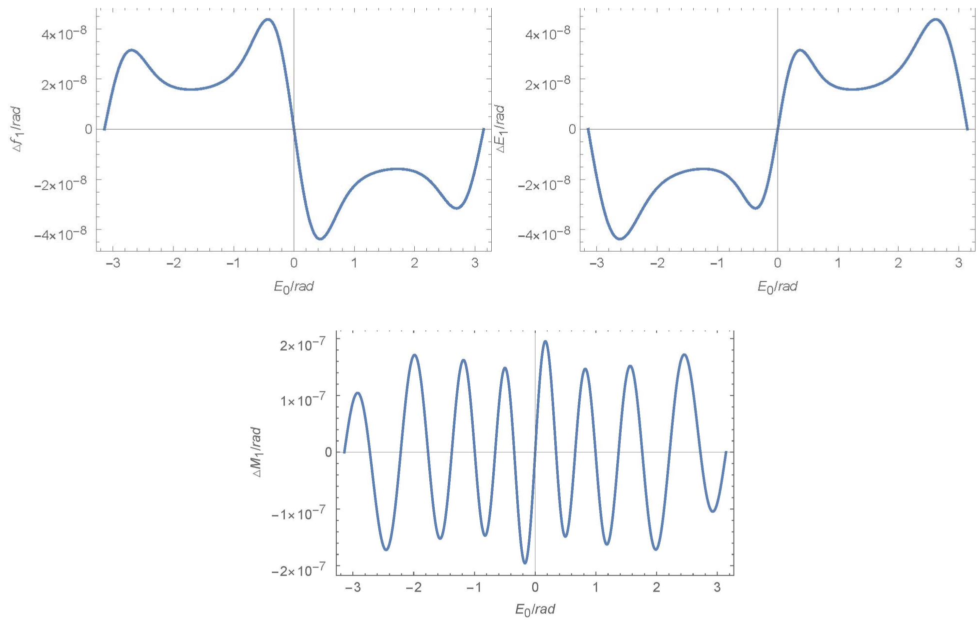

Figure 7. *Cont.*

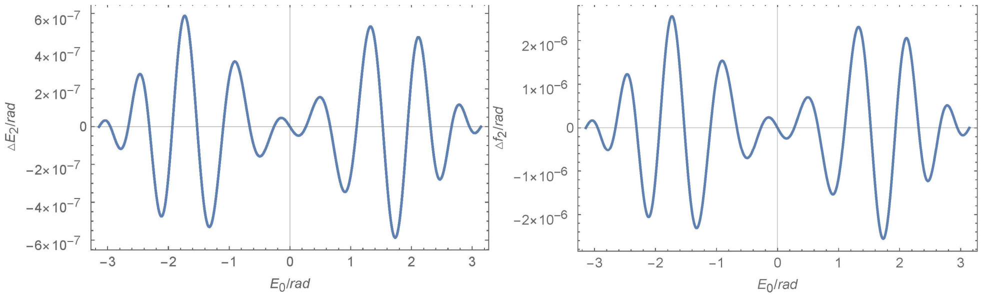

Figure 7. When e = 0.2 and the parameter of the expansion formula is e, the error varies with the elliptic anomaly E_0.

Table 2. The maximum absolute errors of the three types of anomalies under different parameters.

Eccentricities	Parameter	The Maximum Absolute Value of Δf_1/rad	The Maximum Absolute Value of ΔE_1/rad	The Maximum Absolute Value of ΔM_1/rad	The Maximum Absolute Value of ΔE_2/rad	The Maximum Absolute Value of Δf_2/rad
e = 0.01	m	3.8×10^{-16}	3.8×10^{-16}	4.1×10^{-16}	1.5×10^{-16}	4.3×10^{-16}
	e	4.3×10^{-16}	5.0×10^{-16}	4.2×10^{-16}	3.6×10^{-18}	4.3×10^{-16}
e = 0.1	m	4.6×10^{-13}	4.6×10^{-13}	3.6×10^{-11}	3.1×10^{-9}	1.2×10^{-8}
	e	7.6×10^{-11}	7.6×10^{-11}	3.9×10^{-10}	1.2×10^{-9}	5.1×10^{-9}
e = 0.2	m	2.6×10^{-10}	2.6×10^{-10}	2.0×10^{-8}	1.7×10^{-6}	6.6×10^{-6}
	e	4.4×10^{-8}	4.4×10^{-8}	2.0×10^{-7}	5.9×10^{-7}	2.6×10^{-6}

2.6. Symbolic Expression for Extreme Value of Differences among Three Anomalies

2.6.1. Symbolic Expression for Extreme Value of Difference between Elliptic and Mean Anomalies

From Formulas (5), (7), and (8), the derivative of the difference between the elliptic anomaly E and the mean anomaly M with respect to the elliptic anomaly E, the mean anomaly M, and the true anomaly f can be obtained:

$$\frac{d(E-M)}{dE} = e\cos E \tag{33}$$

$$\frac{d(E-M)}{dM} = \frac{e\cos E}{1-e\cos E} \tag{34}$$

$$\frac{d(E-M)}{df} = \frac{\sqrt{1-e^2}e\cos E}{1+e\cos f} \tag{35}$$

By making the above three equations equal to zero and the second derivative not zero, we can obtain the following:

When $E = \frac{\pi}{2}$, $f = +\arccos -e$ (the plus sign indicates an angle range of 0 to 180 degrees. The minus sign indicates an angle range of 180 to 360 degrees), $M = \frac{\pi}{2} - e$, the maximum value of $E - M$ is e.

When $E = -\frac{\pi}{2}$, $f = -\arccos -e$ (the plus sign indicates an angle range of 0 to 180 degrees. The minus sign indicates an angle range of 180 to 360 degrees), $M = -\frac{\pi}{2} + e$, the maximum value of $E - M$ is $-e$.

2.6.2. Symbolic Expression for Extreme Value of Difference between True Anomaly and Elliptic Anomaly

From Formulas (5), (7), and (8), the derivative of the difference between the true anomaly f and the elliptic anomaly E with respect to the elliptic anomaly E, the mean anomaly M, and the true anomaly f can be obtained:

$$\frac{d(f-E)}{dE} = \frac{\sqrt{1-e^2}}{1-e\cos E} - 1 \tag{36}$$

$$\frac{d(f-E)}{dM} = \left(\frac{\sqrt{1-e^2}}{1-e\cos E} - 1\right)\frac{1}{1-e\cos E} \tag{37}$$

$$\frac{d(f-E)}{df} = 1 - \frac{\sqrt{1-e^2}}{1+e\cos f} \tag{38}$$

By making the above three equations equal to zero and the second derivative not zero, we can obtain the following:

$$\cos E = \frac{1-\sqrt{1-e^2}}{e} \tag{39}$$

$$\cos f = \frac{\sqrt{1-e^2}-1}{e} \tag{40}$$

Furthermore, we can obtain the extreme points of three types of anomalies:

$$E = \pm\arccos\frac{1-\sqrt{1-e^2}}{e} \tag{41}$$

$$f = \mp\arccos\frac{\sqrt{1-e^2}-1}{e} \tag{42}$$

$$M = \pm\arccos\frac{1-\sqrt{1-e^2}}{e} \mp \sqrt{2}\sqrt{-1+e^2+\sqrt{1-e^2}} \tag{43}$$

The extreme value is as follows:

$$f - E = \pm\arccos\frac{\sqrt{1-e^2}-1}{e} \mp \arccos\frac{1-\sqrt{1-e^2}}{e} \tag{44}$$

2.6.3. Symbolic Expression for Extreme Value of Difference between True and Elliptic Anomalies

From Formulas (5), (7), and (8), the derivative of the difference between the true anomaly f and the mean anomaly M with respect to the elliptic anomaly E, the mean anomaly M, and the true anomaly f can be obtained:

$$\frac{d(f-M)}{dE} = \frac{\sqrt{1-e^2}}{1-e\cos E} + e\cos E - 1 \tag{45}$$

$$\frac{d(f-M)}{dM} = \frac{\sqrt{1-e^2}}{(1-e\cos E)^2} - 1 \tag{46}$$

$$\frac{d(f-M)}{df} = 1 - (1-e\cos E)\frac{\sqrt{1-e^2}}{1+e\cos f} \tag{47}$$

By making the above three equations equal to zero and the second derivative not zero, we can obtain the following:

$$\cos E = \frac{1-\left(1-e^2\right)^{1/4}}{e} \tag{48}$$

$$\cos f = \frac{-1+\left(1-e^2\right)^{3/4}}{e} \tag{49}$$

Furthermore, we can obtain the extreme points of three types of anomalies:

$$E = \pm\arccos\frac{1-\left(1-e^2\right)^{1/4}}{e} \tag{50}$$

$$f = \pm\arccos\frac{-1+\left(1-e^2\right)^{3/4}}{e} \tag{51}$$

$$M = \mp\sqrt{e^2-\left(1-\left(1-e^2\right)^{1/4}\right)^2} \pm \arccos\frac{1-\left(1-e^2\right)^{1/4}}{e} \tag{52}$$

The extreme value is as follows:

$$f-M = \pm\arccos\frac{-1+\left(1-e^2\right)^{3/4}}{e} \pm \sqrt{e^2-\left(1-\left(1-e^2\right)^{1/4}\right)^2} \mp \arccos\frac{1-\left(1-e^2\right)^{1/4}}{e} \tag{53}$$

The extreme value expression of the differences among the three anomalies obtained above is too complex to have an intuitive understanding of their size relationship. Therefore, the above expression is expressed as a power series with respect to eccentricity e, taken to the 6th order, as shown in the table below.

The following conclusions can be drawn from Table 3:

1. The absolute values of the extreme values of the difference among the three anomalies increase with the increase in eccentricity.
2. The absolute values of the extreme values of the difference $E-M$ between the elliptic anomaly and the mean anomaly, the difference $f-E$ between the true anomaly and the elliptic anomaly, and the difference $f-M$ between the true anomaly and the mean anomaly gradually increase.
3. When the eccentricity is small, the extreme absolute value of the difference $E-M$ between the elliptic anomaly and the mean anomaly, as well as the extreme value of the difference $f-E$ between the true anomaly and the elliptic anomaly, is approximately equal.
4. The absolute value of the extreme value of the difference $f-M$ between the true anomaly and the mean anomaly is approximately twice as large as the absolute value of the extreme value of the difference $E-M$ between the elliptic anomaly and the mean anomaly, and the absolute value of the extreme value of the difference $f-E$ between the true anomaly and the elliptic anomaly.

Table 3. Symbolic expression for extreme value of differences among three anomalies.

Function	Argument	Extreme Point	Extreme Value
$E-M$	E	$\pm\frac{\pi}{2}$	$\pm e$
	M	$\pm\left(\frac{\pi}{2}-e\right)$	
	f	$\pm\left(\frac{\pi}{2}+e+\frac{e^3}{6}+\frac{3e^5}{40}\right)$	
$f-E$	E	$\pm\left(\frac{\pi}{2}-\frac{e}{2}-\frac{7e^3}{48}-\frac{103e^5}{1280}\right)$	$\pm\left(e+\frac{7e^3}{24}+\frac{103e^5}{640}\right)$
	M	$\pm\left(\frac{\pi}{2}-\frac{3e}{2}-\frac{e^3}{48}-\frac{13e^5}{1280}\right)$	
	f	$\pm\left(\frac{\pi}{2}+\frac{e}{2}+\frac{7e^3}{48}+\frac{103e^5}{1280}\right)$	
$f-M$	E	$\pm\left(\frac{\pi}{2}-\frac{e}{4}-\frac{37e^3}{384}-\frac{2363e^5}{40960}\right)$	$\pm\left(2e+\frac{11e^3}{48}+\frac{599e^5}{5120}\right)$
	M	$\pm\left(\frac{\pi}{2}+\frac{3e}{4}+\frac{21e^3}{128}+\frac{3409e^5}{40960}\right)$	
	f	$\pm\left(\frac{\pi}{2}-\frac{5e}{4}-\frac{25e^3}{384}-\frac{1383e^5}{40960}\right)$	

3. Conclusions

This paper establishes a mathematical model for the transformation between the true anomaly and the elliptic anomaly using Lagrange conjugate series. We have redefined the parameters m and used them to represent the relationship between the three anomalies.

In this paper, we iterate over Kepler's equation by using the symbolic iteration method. Then, we derive the series expansion between the mean anomaly and the elliptic anomaly. We can derive the relationship between the mean anomaly M and the true anomaly f by using previous formulas.

By calculating the extreme values of the differences among three anomalies and expanding the extreme values into a power series form of eccentricity e, the form is intuitive and easy to analyze.

Author Contributions: Conceptualization and methodology, D.Z. and S.B.; software, D.Z. and S.B.; validation, D.Z. and H.L.; formal analysis, Y.C.; investigation, W.L.; resources, Y.C.; writing—original draft preparation, D.Z.; writing—review and editing, D.Z.; visualization, D.Z.; supervision, H.L.; project administration, D.Z. All authors have read and agreed to the published version of the manuscript.

Funding: This research was funded by the project from the National Natural Science Foundation of China, grant No. 42074010, grant No. 42174051, and grant No. 42122025.

Institutional Review Board Statement: Not applicable.

Informed Consent Statement: Not applicable.

Data Availability Statement: The data used during the current study are available from the corresponding author on reasonable request.

Acknowledgments: The authors would like to thank the reviewers who gave their valuable suggestions that have helped to improve the quality of the manuscript.

Conflicts of Interest: The authors declare no conflicts of interest.

References

1. Zhao, Q.; Guo, J.; Wang, C.; Lyu, Y.; Xu, X.; Yang, C.; Li, J. Precise orbit determination for BDS satellites. *Satell. Navig.* **2022**, *3*, 1–24. [CrossRef]
2. Chen, G.; Zhou, R.; Hu, Z.; Lv, Y.; Wei, N.; Zhao, Q. Statistical characterization of the signal-in-space errors of the BDS: A comparison between BDS-2 and BDS-3. *GPS Solut.* **2021**, *25*, 112. [CrossRef]
3. Cui, H.; Wang, J.; Wang, M.; Wang, H.; Zhu, W.; Hou, Y. Service Performance Assessment of BDS-3 Using Satellite Distribution Probability. *Geomat. Inf. Sci. Wuhan Univ.* **2021**, *45*, 938–946.
4. Shao, B.; Xin, J.; Lu, H.; Mao, Y.; Yuan, H.; Liu, C.; Hu, X.; Lou, Y. BDS-3 performance assessment: PNT, SBAS, PPP, SMC, and SAR. *Acta Geod. Cartogr. Sin.* **2021**, *50*, 181–193.
5. Li, J. Solar Radiation Pressure Modeling for Beidou-3 Satellites. Ph.D. Thesis, Wuhan University, Wuhan, China, 2022.
6. Yang, Y.; Mao, Y.; Sun, B. Basic performance and future developments of BeiDou global navigation satellite system. *Satell. Navig.* **2020**, *1*, 1. [CrossRef]
7. Han, C.; Liu, L.; Cai, Z.; Lin, Y. The space–time references of BeiDou navigation satellite system. *Satell. Navig.* **2021**, *2*, 18. [CrossRef]
8. Li, P.; Zhang, H. Research on BDS satellites precision orbit determination based on global MGEX observation stations. *J. Navig. Position* **2021**, *9*, 25–32.
9. Gao, D.; Li, H.; Bian, S. The Series Expansions of Transformations between Eccentric, Mean and True Anomalies. *J. Navig. Position* **2015**, *3*, 57–61.
10. Markley, F.L. Kepler Equation solver. *Celest. Mech. Dyn. Astron.* **1995**, *63*, 101–111. [CrossRef]
11. Abubekerov, M.K.; Gostev, N.Y. Solution of Kepler's Equation with Machine Precision. *Astron. Rep.* **2020**, *64*, 1060–1066. [CrossRef]
12. Zhang, R.; Bian, S.; Li, H. Symbolic iteration method based on computer algebra analysis for Kepler's equation. *Sci. Rep.* **2022**, *12*, 2957. [CrossRef] [PubMed]
13. Wu, B.; Zhou, Y.; Lim, C.W.; Zhong, H. A new solution approach via analytical approximation of the elliptic Kepler equation. *Acta Astronaut.* **2023**, *202*, 303–310. [CrossRef]
14. Stumpff, K. *On the Application of Lie—Series to the Problems of Celestial Mechanics*; National Aeronautics and Space Administration: Washington, DC, USA, 1968.
15. Gooding, R.H.; Odell, A.W. The hyperbolic Kepler equation (and the elliptic equation revisited). *Celest. Mech.* **1988**, *44*, 267–282. [CrossRef]
16. Calvo, M.; Elipe, A.; Montijano, J.I. A monotonic starter for solving the hyperbolic Kepler equation by Newton's method. *Celest. Mech. Dyn. Astron.* **2019**, *131*, 18. [CrossRef]
17. Zechmeister, M. Solving Kepler's equation with CORDIC double iterations. *Mon. Not. R. Astron. Soc.* **2021**, *500*, 109–117. [CrossRef]
18. González-Gaxiola, O.; Hernández-Linares, S. An Efficient Iterative Method for Solving the Elliptical Kepler's Equation. *Int. J. Appl. Comput. Math.* **2021**, *7*, 42. [CrossRef]

19. Philcox, O.H.E.; Jeremy, G.; Zachary, S. Kepler's Goat Herd: An exact solution to Kepler's equation for elliptical orbits. *Mon. Not. R. Astron. Soc.* **2021**, *506*, 6111–6116. [CrossRef]
20. Tommasini, D.; Olivieri, D.N. Two fast and accurate routines for solving the elliptic Kepler equation for all values of the eccentricity and mean anomaly. *Astron. Astrophys.* **2022**, *658*, A196. [CrossRef]
21. Bian, S.; Li, H. *Computer Algebra Analysis on Geodesy*, 1st ed.; China Science Publishing & Media Ltd.: Beijing, China, 2018.
22. Li, Q.; Cui, C. *Principles of Satellite Geodesy*, 1st ed.; Surveying and Mapping Publishing: Beijing, China, 1989.
23. Zhao, Y. *Fundamentals of Astromechanics*, 1st ed.; Nanjing University Press: Nanjing, China, 1993.
24. Gu, X. A Calculating Method for Epicyclic Motion of Spacecraft. *J. UEST China* **2003**, *32*, 635–637.
25. Gu, X.; Tan, Z. Calculating Method of Series for the True Anomaly of a Spacecraft Elliptic Orbit. *Appl. Math. Mech.* **2005**, *26*, 45–50. [CrossRef]
26. Liu, L.; Hou, Y. *Fundamentals of Orbital Mechanics*, 1st ed.; Higher Education Press: Beijing, China, 2018.
27. Liu, L. *Orbital Mechanics of Artificial Earth Satellites*, 1st ed.; Higher Education Press: Beijing, China, 1992.
28. Clemence, G.M. *Methods of Celestial Mechanics*, 1st ed.; Academic Press: New York, NY, USA, 1961.
29. Farnocchia, D.; Cioci, D.B.; Milani, A. Robust resolution of Kepler's equation in all eccentricity regimes. *Celest. Mech. Dyn. Astron.* **2013**, *116*, 21–34. [CrossRef]
30. Liu, L. *Theory and Application of Spacecraft Orbit Determination*, 1st ed.; Publishing House of Electronics Industry: Beijing, China, 2015.
31. Liu, L. *Satellite Orbit Theory and Applications*, 1st ed.; Publishing House of Electronics Industry: Beijing, China, 2015.
32. Da, S.F.S. Extension of the solution of Kepler's equation to high eccentricities. *Celest. Mech. Dyn. Astron.* **1994**, *58*, 297–308.
33. Siewert, C.E.; Burniston, E.E. An exact analytical solution of Kepler's equation. *Celest. Mech.* **1972**, *6*, 294–304. [CrossRef]
34. Xiong, J. *Ellipsoidal Geodesy*, 1st ed.; The People's Liberation Army Press: Beijing, China, 1988.
35. Li, Z.; Bian, S.; Kong, H. Symbolic Iterative Method for Solving Inverse Problems in Ellipsoidal Geodesy. *Hydrogr. Surv. Charting* **2013**, *33*, 27–29.
36. Murray, C.D.; Dermott, S.F. *Solar System Dynamics*; Cambridge University Press: Cambridge, UK, 2000.
37. Danby, J.M.A. *Fundamentals of Celestial Mechanics*; Willmann-Bell: Richmond, VA, USA, 1988.
38. Gao, D.; Bian, S.; Li, H. Symbolic Expressions of Difference Extrema Between Anomalies for Satellite Movement. *Hydrogr. Surv. Charting* **2015**, *35*, 8–11.